# Molecular Orientation Distributions in Protein Films: III. Yeast Cytochrome *c* Immobilized on Pyridyl Disulfide-Capped Phospholipid Bilayers

Paul L. Edmiston and S. Scott Saavedra
Department of Chemistry, University of Arizona, Tucson, Arizona 85721 USA

ABSTRACT Molecular orientation in a hydrated monolayer film of yeast cytochrome *c,* immobilized via disulfide bonding between Cys-102 and a pyridyl disulfide-capped phospholipid bilayer deposited from an air-water interface onto glass substrates, was investigated. The orientation distribution of the heme groups in the protein film was determined using a combination of absorption linear dichroism, measured in a planarintegrated optical waveguide-attenuated total reflection geometry- and fluorescence anisotropy, measured in a total internal reflection geometry. A gaussian model for the orientation distribution was used to recover the mean heme tilt angle and angular distribution about the mean, which were 40 and 11°, respectively. Additional experiments showed that a large fraction of the cytochrome *c* was disulfide bonded to the bilayer, which correlates with the high degree of macroscopic order in the protein film. However, a subpopulation of yeast cytochrome *c* molecules in the film (~30% of the total) appeared to be nonspecifically adsorbed. The orientation distribution of this subpopulation was found to be much broader than the specifically bound fraction.

## INTRODUCTION

Immobilization of protein film assemblies on solid substrates is of widespread interest because they are a key component in molecular devices such as biosensors (Swalen et al., 1987; Arnold and Meyerhoff, 1988) and affinity-based chromatographic supports (Hage and Kao, 1991; De Ruiter, 1992). In general, the ligand binding site(s) comprises a relatively small fraction of the total surface area of a protein. As a result, the active site of a protein molecule, when immobilized on a solid support, can be sterically inaccessible to a dissolved ligand, impairing the bioactivity of the protein. Observed differences in surface activity and bioactivity among protein-surface combinations have frequently been attributed to differences in molecular orientation (Darst et al., 1988; Tarlov and Bowden, 1991; Hamachi et al., 1991; Müller et al., 1993; Cullison et al., 1994). Consequently, the development of methodologies to attach a protein via a structurally unique site to a functionalized surface to produce a geometrically defined orientation has been a focus of considerable research efforts in recent years (Blankenburg et al., 1989; Pachence and Blasie, 1991; Fraaije et al., 1990; Timbs and Thompson, 1990; Song et al., 1993, Prokop et al., 1995; Mrksich et al., 1995; Firestone et al., 1996).

In order to assess the results of immobilization methodologies, analytical techniques must be available to measure the surface coverage, orientation distribution, conformational distribution, and biological activity of noncrystalline protein assemblies. Orientation has received little attention due to the technical difficulty of measuring this parameter in a monolayer or less of protein located at a solid-liquid interface. Recently, we reported a method based on a combination of two techniques, absorbance linear dichroism measured in a planar integrated optical waveguide-attenuated total reflection (IOW-ATR) geometry and emission anisotropy measured in a total internal reflection fluorescence (TIRF) geometry, to determine the orientation distribution of porphyrin groups in an immobilized heme protein film (Edmiston et al., 1997). From these measurements, the mean heme tilt angle and angular distribution about the mean are calculated by modeling the distribution as a gaussian function. The theory and initial application of the IOW-ATR + TIRF technique are described elsewhere (Edmiston et al., 1997).

The use of a unique cysteine to covalently anchor a heme protein in a site-directed manner to a modified surface has been reported elsewhere (Pachence et al., 1990, Firestone et al., 1996). Martin et al. (1981) used this approach to covalently bond antibody Fab fragments to liposomes for the purposes of drug delivery. The first orientation distribution measurements on protein films immobilized via a cysteine-directed chemistry were recently reported from this laboratory (Wood et al., 1997). In this work we use the IOW-ATR + TIRF technique to determine the molecular orientation distribution of wild type yeast iso-1-cytochrome *c* immobilized on a pyridyl disulfide-capped, phospholipid bilayer (Fig. 1) deposited on a planar support by the Langmuir-Blodgett (LB) method. Immobilization of the protein is accomplished by forming a disulfide bond between the single reduced cysteine at position 102 and the pyridyl disulfide reactive group. The results show that a majority of the cytochrome *c* molecules in a film produced by this site-directed methodology are covalently bound, resulting in

*Received for publication 4 April 1997 and in final form 9 November 1997.*
Address reprint requests to Dr. S. Scott Saavedra, Department of Chemistry, University of Arizona, Tucson, AZ 85721. Tel.: 520-621-9761; Fax: 520-621-8407; E-mail: saavedra@u.arizona.edu.

0006-3495/98/02/999/08 $2.00

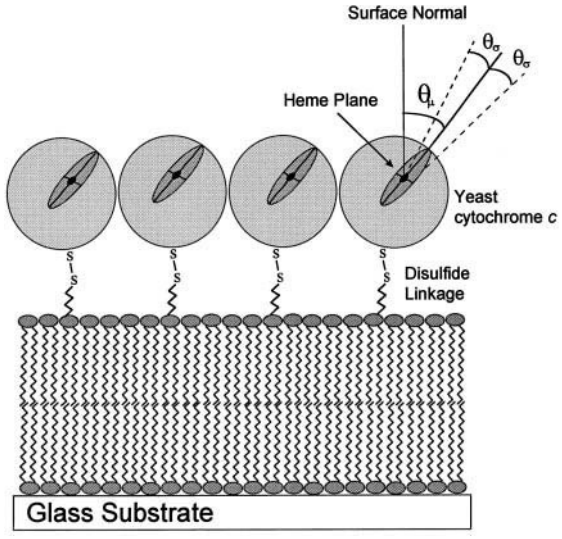


FIGURE 1 Schematic of the immobilized protein film architecture under study. A phospholipid bilayer consisting of a 1:8 mol/mol ratio of DOPE-PDS:DOPC is first deposited onto a bare glass substrate using the Langmuir-Blodgett method. Wild type yeast cytochrome *c* is covalently bound to the PDS moiety on the lipid bilayer surface via a reduced cysteine at position 102. Orientation measurements used the heme as an intrinsic spectroscopic probe. The mean orientation of the heme groups is described by $\theta_\mu$, which is the tilt angle between film surface normal and the heme molecular plane. The distribution of tilt angles about the mean is $\theta_\sigma$, the standard deviation of the gaussian distribution function that is assumed to approximate the true orientation distribution.

a narrow orientation distribution (i.e., a macroscopically ordered film).

## MATERIALS AND METHODS

### Protein solutions

Yeast cytochrome *c* (Sigma, St. Louis, MO, Type I) from *Saccharomyces cerevisiae* was dissolved in 50 mM citrate buffer, pH 6.0, containing 100 mM KCl (citrate buffer). A molar excess of dithiothreitol (DTT, Sigma, 99%) was added to reduce the protein to ferrocytochrome *c* (cyt *c*) and eliminate protein dimers. Excess DTT was removed by purification on a Sephadex G-25 column, and the concentration of the cyt *c* stock solution was measured using absorbance spectrometry ($\epsilon_{408}$ = 96,000 $M^{-1}$ $cm^{-1}$). These solutions were used immediately after preparation.

The iron complexed in the heme of native cyt *c* effectively quenches porphyrin fluorescence. To perform anisotropy measurements, the iron was replaced with zinc to yield a fluorescent, zinc-substituted cyt *c* (Zn-cyt *c*). Zn-cyt *c* was prepared as described previously (Edmiston et al., 1997) by first removing the native iron (Robinson and Kamen, 1968). The only modification of this procedure was that the final dialysis of Zn-cyt *c* was performed against citrate buffer. This modification was used because precipitation of the protein was occasionally observed at pH 7. The concentration of Zn-cyt *c* solutions was determined by absorbance spectrometry using $\epsilon_{420}$ = 112,000 $M^{-1}$ $cm^{-1}$. (The molar absorptivity was measured by two independent methods. In the first, a direct measurement was performed after lyophilizing the protein from deionized water. In the second, a standard bicinchoninic acid protein assay (Smith et al., 1985) was performed. Both measurements yielded the same result.) Just prior to use, stock solutions of Zn-cyt *c* were treated with excess DTT and purified on a Sephadex G-25 column to eliminate protein dimers that may have formed during storage. Solutions were used immediately after purification.

### Langmuir-Blodgett film deposition

LB deposition of phospholipid bilayers was carried out with some modifications of the procedure described by Tamm and McConnell (1985). Fused quartz slides (2.5 cm × 7.5 cm × 1 mm thick, Heraeus, Duluth, GA) were used as substrates for TIRF anisotropy measurements. Silica-titania waveguides fabricated by a sol-gel dip-coating process (Yang et al., 1994) were used as substrates for IOW-ATR linear dichroism experiments. All substrates were cleaned prior to deposition by soaking in an 80°C chromic acid bath for 30 min, rinsing with deionized water (type 1 reagent grade), scrubbing lightly with a cotton pad in 0.1% PCC-54 surfactant (Pierce, Rockford, IL), and again rinsing with deionized water. The substrates were blown dry with $N_2$ prior to use.

A spreading solution consisting of a 1:8 molar ratio of 1,2-dioleoyl-*sn*-glycero-3-phosphoethanolamine-*N*-[3-(2-pyridyldithio)propionate] (DOPE-PDS, Avanti, Alabaster, AL) and 1,2-di[cis-9-octadecenoyl]-*sn*-glycero-3-phosphocholine (DOPC, Sigma, 99%) was prepared in chloroform (HPLC grade, Aldrich, Milwaukee, WI, 99.9%+) at a total lipid concentration of 3 mg/ml. Structures of these lipids are shown in Fig. 2. The 1:8 molar ratio of DOPE-PDS:DOPC was selected based on: 1) a surface area per lipid molecule of 65 $Å^2$ (as determined by a surface area-pressure isotherm; see below), which corresponds to one DOPE-PDS molecule per 585 $Å^2$ and 2) a surface coverage of $2.2 \times 10^{-11}$ mol/$cm^2$ for a close packed cyt *c* monolayer (Edmiston et al., 1997), which corresponds to a projected area of 755 $Å^2$ per protein molecule. Thus, the molar ratio of cyt *c* to DOPE-PDS is predicted to be no greater than 0.8.

LB films were deposited using a NIMA Technology Model 611 trough. Two slides were placed back-to-back, mounted on the dipping mechanism, and immersed in a subphase of type I deionized water. The use of two slides allowed for LB film deposition on only one side of each slide. Sufficient spreading solution was added to the trough surface and the chloroform was allowed to evaporate. The film was initially compressed to 5 mN/m and allowed to equilibrate for 15–20 min. Compression to the deposition pressure of 35 mN/m was then performed at a rate of 50 $cm^2$/min, and the film was again allowed to equilibrate for 5 min. Vertical deposition was performed at a dipping rate of 2 mm/min and a subphase temperature of 21°C. Transfer ratios between 1 and 1.1 were consistently measured for the first layer. The second monolayer was deposited in a horizontal geometry. The pair of slides were remounted on the dipper arm with the slide plane parallel to the surface of the trough. With the surface pressure held constant at 35 mN/m, the slides were pushed horizontally through the surface of the trough at a velocity of 100 mm/min. At this

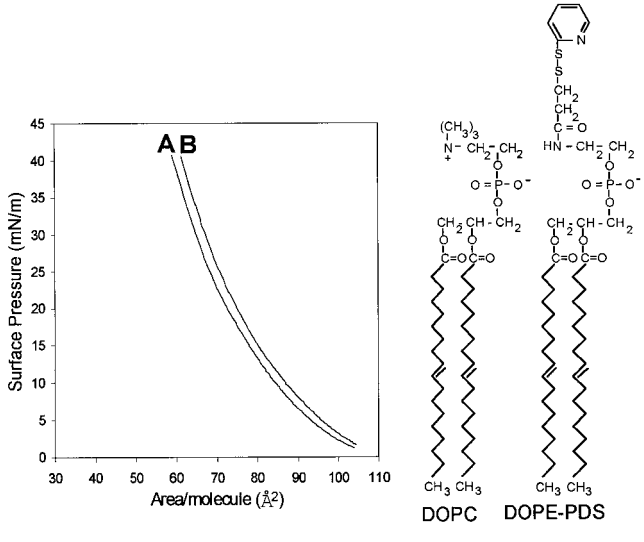


FIGURE 2 Pressure area isotherms of for: (*A*) DOPC and (*B*) 1:8 DOPE-PDS:DOPC on a subphase of type 1 deionized water at a temperature of 21°C. The structures of DOPC and DOPE-PDS are also shown.

point, the lower slide supporting the phospholipid bilayer film was removed from the dipper and transferred to a collection dish placed in the trough prior to the addition of the subphase. The upper slide, having only a monolayer phospholipid film deposited from the vertical transfer step, was discarded. The substrate supporting the phospholipid bilayer was removed from the trough and mounted in a flow cell without exposure to air.

To assess the macroscopic uniformity of these films, phospholipid bilayers consisting of DOPC doped with a 0.7% molar ratio of the fluorescent lipid 1-acyl-2-[12-[(7 nitro-2-1,3-benzoxadiazol-4-yl)amino]dodecanoyl]-*sn*-glycero-3-phosphoethanolamine (NBD-PE, Avanti) were also prepared.

## Orientation measurements

IOW-ATR linear dichroism measurements and TIRF anisotropy measurements were performed as described previously (Edmiston et al., 1997). Orientation measurements were performed on films incubated with either 35 $\mu$M cyt *c* (for IOW-ATR) or 35 $\mu$M 1:5 mol/mol Zn-cyt *c*:cyt *c* (for TIRF). In the latter case, cyt *c* was used as a diluent to increase the separation distance between adsorbed Zn-cyt *c* molecules. The $\alpha/\beta$ absorption bands of ferrocytochrome *c* do not overlap the Zn-cyt *c* emission band centered near 620 nm (Edmiston et al., 1997). Thus, assuming a statistical arrangement of protein molecules in a packed monolayer, the distance between Zn-cyt *c* molecules is sufficient to minimize nonradiative energy, which could result in depolarized fluorescence emission.

Protein solutions were injected into the flow cell and incubated with the supported lipid bilayer for a period of 14 h. The time period was chosen to ensure complete reaction between cyt *c* and DOPE-PDS based on previous kinetic experiments (Martin et al., 1981). After 14 h, the protein incubation solution was flushed from the flow cell using citrate buffer followed by spectroscopic measurements. Three replicates were performed for both the linear dichroism and anisotropy experiments. Orientation distributions were calculated using a gaussian model as described previously (Edmiston et al., 1997) and reported as a mean and standard deviation ($\theta_\mu \pm \theta_\sigma$).

## Protein surface coverage determination

The surface coverage of cyt *c* immobilized on DOPE-PDS/DOPC bilayers was determined using a surfactant desorption assay. This procedure was carried out by first depositing phospholipid bilayers on three 3 × 2-inch glass microscope slides using the same deposition procedure described above. The supported bilayers were transferred without exposure to air to an incubation cell containing 50 ml of buffer. The buffer solution was then exchanged for a 35-$\mu$M 1:4 mol/mol Zn-cyt *c*:cyt *c* solution and incubated under conditions equivalent to those used to form protein films for orientation measurements. After incubation, the slides were rinsed with buffer and placed in a teflon container containing 12.5 ml of buffer/surfactant solution (50 mM citrate buffer, pH 6.0, containing 200 mM KCl and 1% (v/v) Triton X-100). All three slides were placed in this solution to increase the concentration of desorbed protein. The teflon cell containing the slides and surfactant solution was sonicated for ~10 min to dissolve the bilayers and associated protein. Essentially quantitative desorption of the protein via this treatment was confirmed by epifluorescence microscopy.

The amount of desorbed protein was quantitated using an external calibration curve. A dilution series of Zn-cyt *c* was prepared using the same buffer/surfactant solution that was used to remove lipid bilayers and protein from the slides. The dilution series also contained lipids equal in composition and concentration to those that comprised the dissolved bilayers. The surface coverage was calculated by ratioing the amount of desorbed protein to the area of the slides, assuming an atomically flat glass surface and a value of $2.2 \times 10^{-11}$ mol/cm$^2$ for the surface density of a close packed cyt *c* monolayer (Edmiston et al., 1997).

## Protein desorption experiments

Protein films were prepared as described above using the 35 $\mu$M 1:5 Zn cyt *c*:cyt *c* solutions used for fluorescence anisotropy experiments. Two types of planar bilayers were used as adsorbent surfaces: pure DOPC serving as a control and 1:8 DOPE-PDS:DOPC. The amount of protein removed from the surface of phospholipid bilayers by incubation in a variety of desorption solutions was analyzed using epifluorescence microscopy, as described previously (Edmiston et al., 1997). Briefly, after rinsing the protein film with 50 mM citrate buffer containing 100 mM KCl, an initial mean emission intensity was obtained by measuring fluorescence from five widely spaced spots on each film. In subsequent steps, citrate buffer containing either 200 mM KCl or 10 mM DTT or both was added to the flow cell, incubated for a prescribed time, and then rinsed with citrate buffer. The mean emission intensity of the film was measured after each treatment, ratioed to the initial mean intensity, and reported as a percentage. It was assumed that differences in solution composition had no effect on the molar absorptivity and quantum yield of immobilized Zn-cyt *c*.

# RESULTS AND DISCUSSION

## LB film characterization

The pressure area isotherms of pure DOPC and a 1:8 mol/mol DOPE-PDS:DOPC mixture measured at 21°C are shown Fig. 2. Both curves depict a single fluid phase. This is characteristic of DOPC, which has a chain-melting temperature of −22°C. The isotherm of the mixture was nearly identical in shape to pure DOPC. The slight increase in area/molecule versus pressure observed for the DOPE-PDS/DOPC mixture may be due to the bulkier PDS headgroups. Deposition at 35 mN/m corresponds to mean molecular area of approximately 65 Å$^2$, a typical value for a fluid, packed monolayer (Luzzati, 1968; Yue et al., 1976; Tamm and McConnell, 1985).

To assess the macroscopic uniformity of lipid bilayers, a small amount of fluorescently labeled lipid (NBD-PE) was introduced into 1:8 mol/mol DOPE-PDS:DOPC films and observed using an epifluorescence microscope. The NBD-PE-doped films were used for characterization purposes only. Spatially uniform fluorescence was observed at a magnification of 400×, indicating a lack of micron-scale defects or phase differences within the film structure (Helm et al., 1987). After incubation overnight with either 2 mg/ml bovine serum albumin or 10 mM DTT in 50 mM citrate buffer, NBD-doped bilayers were unaltered as determined by both visual inspection of uniformity and quantitative measurements of the emission intensity. Rinsing with buffer also did not affect uniformity or emission intensity. To determine whether lateral diffusion was occurring within the bilayer, a small area was photobleached using epi-illumination focused with 40× objective for 15 s. Fluorescence intensity was then qualitatively observed at lower magnification; the photobleached hole contracted steadily until finally disappearing after roughly 30 min. This qualitative result is consistent with diffusion coefficients on the order of $10^{-8}$ cm$^2$/s measured on similar films using fluorescence recovery after photobleaching (Tamm and McConnell, 1985).

## Protein film characterization

Zn-cyt *c*-doped protein films prepared for TIRF anisotropy measurements were also examined using epifluorescence microscopy. Emission from protein films appeared spatially uniform, lacking any macroscopic features. This observation was confirmed by TIRF measurements; the fluorescence emission measured at five widely spaced locations in each film varied by a maximum of 6% (relative standard deviation). The surface coverage of cyt *c* immobilized on 1:8 DOPE-PDS:DOPC films was measured using a surfactant desorption assay. A surface coverage of $2.0 \times 10^{-11}$ mol/cm$^2$ was obtained. This value corresponds to 0.9 monolayer based on a surface coverage of $2.2 \times 10^{-11}$ mol/cm$^2$ for a close-packed cyt *c* monolayer (Edmiston et al., 1997), which assumes that the orientation of the molecules in the film is geometrically random and no spreading occurs due to denaturation that might be induced by adsorption.

## Orientation measurements

The dichroic ratio ($\rho$) and anisotropy ($r$) measurements performed on yeast cyt *c* films formed on DOPE-PDS:DOPC lipid bilayers yielded values of $1.13 \pm 0.10$ and $-0.101 \pm 0.012$, respectively ($n = 3$ for both). From the mean values, an orientation distribution ($\theta_\mu \pm \theta_\sigma$) of $40 \pm 11$ degrees was calculated based on a gaussian distribution model. The normalized distribution is plotted in Fig. 3. The molecular geometry is depicted schematically in Fig. 1 in which $\theta_\mu = 40°$ is the mean tilt angle between the surface normal and the heme plane.

It is appropriate to consider the effect of measurement errors on the calculated orientation distribution. This is illustrated in a limited manner in Table 1 in which calculated distributions are listed for a range of values for dichroic ratio ($\rho$) and anisotropy ($r$) within one standard deviation of the respective means of 1.13 and $-0.101$. This table

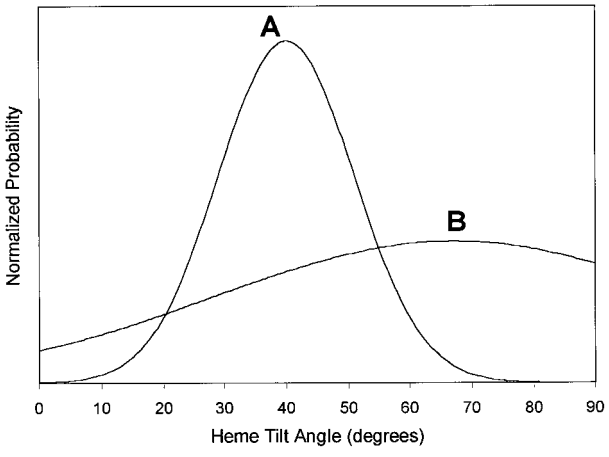


FIGURE 3 Gaussian probability distributions for: (*A*) yeast cyt *c* immobilized on pyridyl disulfide-capped phospholipid bilayers; $\theta_\mu = 40°$ and $\theta_\sigma = 11°$. (*B*) yeast cyt *c* immobilized on thiol terminated, self-assembled monolayers (Wood et al., 1997); $\theta_\mu = 67°$ and $\theta_\sigma = 11°$.

**TABLE 1 Gaussian orientation distributions calculated for selected combinations of emission anisotropy and dichroic ratio**

| | Anisotropy | | |
|---|---|---|---|
| Dichroic ratio | −0.082 | −0.101 ± 0.012* | −0.113 |
| 1.03 | 37 ± 10 | n/o | n/o |
| 1.08 | 38 ± 6 | 39 ± 14 | 42 ± 20 |
| 1.13 ± 0.1* | 42 ± 2 | 40 ± 11 | 41 ± 15 |
| 1.18 | n/o | 41 ± 6 | 41 ± 11 |
| 1.23 | n/o | n/o | 41 ± 7 |

*Overall measured mean and standard deviation for yeast cyt *c* bound to 1:8 DOPE-PDS:DOPC planar-supported lipid bilayers.
n/o, not obtainable. The pair of values is physically inconsistent with a Gaussian orientation distribution of circularly polarized oscillators.

demonstrates two points. First, for some pairs of $\rho$ and $r$ values, an orientation distribution cannot be calculated because the values are theoretically inconsistent. This is an example of the cross-checking nature provided by performing two individual experiments to arrive at an orientation distribution (Edmiston et al., 1996); only limited number of combinations of $\rho$ and $r$ are theoretically self-consistent. Second, the calculated orientation distributions do not vary appreciably within one standard deviation of the mean $\rho$ and $r$ values; the narrowest distribution is $42 \pm 2°$ while the broadest is $42 \pm 20°$. The distribution calculated from the mean values, $40 \pm 11°$, appears to be representative of the distributions listed in Table 1.

Based on a model of yeast cyt *c* disulfide bonded to an extrinsic sulfhydryl group, an orientation distribution centered about 40° is geometrically reasonable. The Cerius$^2$ software (BioSym/Molecular Simulations Inc., San Diego, CA) package was used to construct the model that consisted of a single yeast cyt *c* molecule covalently bound via Cys-102 to a planar phospholipid layer composed of 1:8 DOPE-PDS:DOPC with a packing density of 65 Å$^2$/lipid. Bond lengths, angles, torsions, and inversions were minimized using the software package. Hydrogen bonding and van der Waals interactions were also minimized using a DREIDING force field (Mayo et al., 1990). The angle between the heme plane and the normal axis to the lipid surface plane in the model was 32°, which agrees reasonably well with the experimental value of 40°. However, it is important to note that since parameters such as solvent molecules, neighboring cyt *c* molecules, and electrostatic terms were omitted, the model does not represent a theoretical simulation of the environment that would be experienced by an immobilized cyt *c* molecule.

## Desorption experiments

To assess the types of interactions that immobilize cyt *c* to the phospholipid bilayers used here, a series of desorption experiments was performed. The data (Table 2) reveal that a disulfide bond is not the sole interaction between cyt *c* and the lipid bilayer surface. Approximately 10% of the cyt *c*

**TABLE 2 Desorption of yeast cyt *c* from planar lipid bilayers by salt and dithiothreitol solutions**

| Desorption treatment | Percentage of initial fluorescence intensity after applying desorption treatments to cyt *c* films*immobilized on bilayers composed of: DOPC (%) | 1:8 DOPE-PDS:DOPC (%) |
|---|---|---|
| Buffer rinse (50 mM citrate buffer, pH 6.0, 100 mM KCl) | 100 | 100 |
| Buffer containing 200 mM KCl, 15-min static incubation | 51 ± 1 ($n$ = 2) | 91 ± 5($n$= 7) |
| Buffer containing 10 mM DTT, 15-min static incubation | 47 ($n$ = 1) | 58 ± 5($n$=5)§ |
| Buffer containing 200 mM KCl, 10 mM DTT, 15-min static incubation | nm# | 41 ± 2($n$=2)¶ |
| Buffer containing 10 mM DTT, 24-h static incubation | nm | 36 ± 2($n$=3)§ |
| Buffer containing 200 mM KCl, 10 mM DTT, 24-h static incubation | nm | 32 ± 4($n$=4)¶ |
| Buffer containing 200 mM KCl, 24-h static incubation | 25 ± 5 ($n$ = 2) | nm |

*Protein films were formed by treatment of surfaces with 1:5 Zn cyt *c*:ferrocyt *c* under the same conditions used to form films for orientation distribution measurements (see text). Epifluorescence emission intensities measured after application of each desorption treatment were normalized to the first value measured for each film after the initial rinse in phosphate buffer.

#Not measured.

§¶Denotes separate series of sequential desorption experiments.

immobilized on DOPC:DOPE-PDS bilayers was removed by incubation in buffer containing 200 mM KCl, which indicates that a small fraction of the protein layer is electrostatically adsorbed. To determine the extent of covalent bond formation between cyt *c* and PDS lipids, a 10 mM solution of DTT was added to the flow cell. About 42% of the protein was removed by this sequential treatment after 15 min, and ~64% was removed during a 24 h incubation, leaving ~36% of the protein still immobilized to the bilayer surface. It was hypothesized that although a disulfide bond was being cleaved by DTT treatment, an electrostatically mediated interaction between cyt *c* and the bilayer prevented desorption. To test for possible secondary electrostatic interactions, desorption experiments were performed in which protein/DOPE-PDS:DOPC films were treated with citrate buffer containing both 10 mM DTT and 200 mM KCl. Only a slightly greater percentage of immobilized protein was removed by the combined treatment: 59% after 15 min and 68% after 24 h. In summary, the desorption experiments indicate that in a yeast cyt *c* film bound to a 1:8 DOPE-PDS:DOPC lipid bilayer, ~10% of the molecules are electrostatically adsorbed, and ~60% are covalently attached via disulfide bonding. The remaining 30% are bound by unknown interactions; for purposes of additional discussion, this latter fraction is referred to below as the irreversibly bound fraction.

At neutral pH, DOPE-PDS has a charge of −1, whereas cyt *c* has a charge of about +8 that is asymmetrically distributed over the surface of the protein (Brayer and Murphy, 1996). Thus, the observation of electrostatic adsorption of cyt *c* to a DOPE-PDS:DOPC bilayer is not surprising. However, control experiments showed that cyt *c* also adsorbed to pure DOPC bilayers and that the extent of adsorption was substantial. Specifically, the emission intensities of zinc cyt *c*:cyt *c* films adsorbed from 35 $\mu$M protein solutions on pure DOPC and 1:8 DOPE-PDS:DOPC bilayers were approximately equal. However, in contrast to the results obtained for the mixed bilayer, ~75% of the protein adsorbed to a pure DOPC bilayer could be removed by soaking the film in 200 mM KCl for 24 h (Table 2). It is interesting to note that the remaining fraction (~25%) is similar in magnitude to the irreversibly bound fraction observed with the mixed bilayer. These results show that the contribution of the DOPE-PDS dopant to nonspecific cyt *c* adsorption on mixed bilayers was minimal. This conclusion is supported by the surface coverage data from which a molar ratio of DOPE-PDS to immobilized cyt *c* of 1.4 was determined. This ratio is too low to support formation of a multidentate electrostatic interaction between cyt *c* and the LB film, which is thought to be the mechanism of strong cyt *c* adsorption to polyanionic surfaces (Sankaram and Marsh, 1993; Tarlov and Bowden, 1991; Pachence et al., 1990; Muga et al., 1991).

The extent of the (apparently) electrostatic interaction between pure DOPC bilayers and yeast cyt *c* is somewhat surprising given the zwitterionic nature of the phosphatidylcholine headgroup. In contrast, the adsorptive interaction between phosphatidylcholine membranes and horse heart cytochrome *c* (which is structurally very similar to yeast cyt *c*) is weak (Salamon and Tollin, 1996) or nonexistent (Quinn and Dawson, 1969; Demel et al., 1989; Sankaram and Marsh, 1993).

The negatively charged glass substrate supporting the bilayer is one possible cause of an electrostatic attraction between yeast cyt *c* and DOPC. The energy of this interaction is a function of the charge density on the substrate surface and the distance between the substrate and the protein. A charge density of 0.41 charges/nm$^2$ for silica was measured in the presence of 1 N $NaClO_4$ at pH 7.0 (Schindler et al., 1976); a similar value was measured for quartz (Alhmed, 1966). These results were confirmed by capillary electrophoresis studies (Kohr and Engelhardt, 1993; Huang et al., 1996). Deposition of a DOPC bilayer on silica would generate eight positive and eight negative charges per negative charge on the silica surface. Thus, the charge density in the bilayer should screen the silica surface charge density. Distance is another factor that should minimize the interaction. From Coulomb's law, the electrostatic potential due to

the glass surface should be substantially negated due to the bilayer thickness (~45 Å) (Wiener and White, 1992). In summary, the apparently electrostatic interaction that occurs between DOPC bilayers and yeast cyt *c* cannot be ascribed to the negative charge on the substrate. At this time, the mechanism of this adsorption remains unclear.

### Irreversibly immobilized protein

The desorption experiments showed that irreversibly bound protein molecules comprise about 30% of the near-monolayer yeast cyt *c* film immobilized on a DOPE-PDS:DOPC bilayer. The molecular interactions that immobilize this subpopulation of protein molecules are unknown; possible explanations include: 1) disulfide bonds inaccessible to DTT; 2) hydrophobic interactions with alkyl lipid chains, which could result from penetration of the protein into the bilayer (note that hydrophobic interactions were not addressed by the desorption experiments); or 3) a combination of 1 and 2.

In order to examine the influence of the irreversibly bound protein fraction on the orientation distribution measured for the entire film (defined as 0.9 monolayer), the orientation distribution of the irreversibly bound fraction was measured. We assume that the orientation distribution of the entire film is composed of submonolayer fractions, each having a respective orientation distribution. When the film contains two subpopulations of protein molecules, the orientation distribution of the entire film, $N(\theta)_{\text{total}}$, is given by

$$N(\theta)_{\text{total}} = A(N(\theta)_{\alpha}) + B(N(\theta)_{\beta}) \quad (1)$$

in which the $N(\theta)_{\alpha}$ and $N(\theta)_{\beta}$ are the orientation distributions of subpopulations $\alpha$ and $\beta$, respectively. The quantities $A$ and $B$ represent respectively the fractions of the protein film that are irreversibly adsorbed ($A$) and can be desorbed in the presence of salt and DTT ($B$), so $A + B = 1$.

Neglecting orientation effects, the fluorescence intensities measured in the desorption experiments were used to estimate $A = 0.3$ and $B = 0.7$. To determine the orientation distribution of fraction $\alpha$, immobilized cyt *c* films were prepared under conditions identical to those described above and were subjected to a 24 h desorption treatment in a buffer solution containing 200 mM KCl and 10 mM DTT, which removed the covalently and electrostatically bound fraction (~70%) of the protein film. Measurements of anisotropy and linear dichroism on the remainder (~30%) of the film yielded values of $-0.097 \pm 0.017$ ($n = 3$) and 0.965 ($n = 1$), respectively. From these parameters, an orientation distribution of $33 \pm 40°$ was calculated for fraction $\alpha$. This distribution is much broader than the distribution determined for the entire film ($40 \pm 11°$), which shows that the irreversibly bound subpopulation is relatively disordered.

To recover the orientation distribution of fraction $\beta$, the distribution function for fraction $\alpha$ was substituted into Eq. 1 along with values of $A = 0.3$ and $B = 0.7$. This expression for $N(\theta)_{\text{total}}$ was then substituted into the expressions that relate anisotropy and dichroic ratio to molecular orientation distribution in an ensemble of circularly polarized oscillators (Eqs. 4–7 in Edmiston et al., 1997). Using $r = -0.101$ and $\rho = 1.12$, respectively, for the anisotropy and dichroic ratio of the entire film, an orientation distribution of $39 \pm 9°$ was recovered for fraction $\beta$. This distribution is narrower that the orientation distribution of the entire film, as Fig. 4 illustrates. However, the difference is small as fraction $\alpha$ accounts for only 30% of the entire film, and the means of the two subpopulations are not significantly different.

The preceding paragraphs demonstrate that it is possible to measure orientation distributions of subpopulations in a hydrated protein monolayer if: 1) a methodology is available to selectively desorb individual subpopulations from the entire film and 2) a technique with sufficient sensitivity to measure absorbance linear dichroism on submonolayer films is available. Here the sensitivity was provided by the planar waveguide-attenuated total reflection geometry. However, it should be emphasized that although our measurements of orientation distributions of film subpopulations is revealing, the results should be considered preliminary as the dichroic ratio of fraction $\alpha$ was measured on only one sample.

### Assessment of the site-directed methodology

In a previous study (Edmiston et al., 1997), adsorption of horse heart cytochrome *c* to arachidic acid LB films was found to produce a highly ordered protein film in which the orientation distribution of the porphyrin groups was $46 \pm 6°$. The narrow orientation distribution was thought to be the result of a site-directed, electrostatically mediated adsorption mechanism. In the present study, yeast cyt *c* immobilized on DOPE-PDS:DOPC bilayers produced a com-

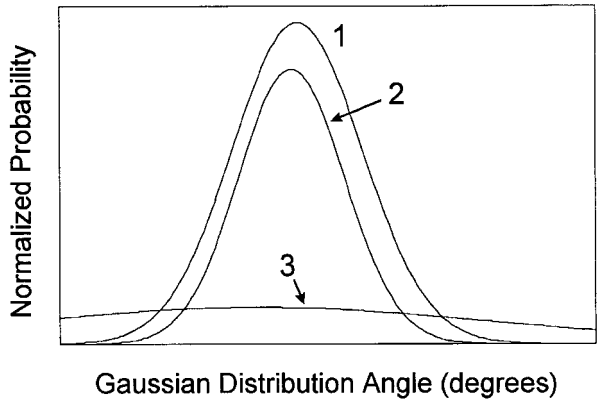


FIGURE 4 Gaussian probability distributions for yeast cyt *c* molecules bound to pyridyl disulfide capped phospholipid bilayers. (*1*) entire film; $\theta_{\mu} = 40°$ and $\theta_{\sigma} = 11°$. (*2*) subpopulation composed of covalently bonded and electrostatically adsorbed molecules consisting of 70% of the film; $\theta_{\mu} = 39°$ and $\theta_{\sigma} = 9°$. (*3*) subpopulation of irreversibly bound protein molecules consisting of 30% of the film; $\theta_{\mu} = 33°$ and $\theta_{\sigma} = 40°$.

parably narrow distribution of 40 ± 11°. This result correlates with a majority of protein molecules in the film being immobilized to the PDS moieties via a site-directed, covalent bond.

In contrast, a similar site-directed, covalent bonding strategy used in a previous study (Wood et al., 1997) produced a relatively disordered protein film. Wild-type yeast cyt *c* was immobilized on thiol-terminated, self-assembled monolayers (SAMs), which produced a porphyrin orientation distribution of 67 ± 39°. Fig. 3 illustrates the difference between the orientation distributions in yeast cyt *c* films deposited on the lipid- and SAM-based architectures. Desorption experiments performed on the SAM-based films (analogous to the desorption experiments described above) showed that the broad orientation distribution was attributable to extensive nonspecific binding which occurred between the protein and the SAM surface. Moreover, little cyt *c* was found to be immobilized to the thiol-capped SAM solely via a disulfide bond.

In the present study, a zwitterionic phospholipid bilayer was used as the primary component of the adsorbent to eliminate nonspecific interactions that could potentially compete with site-directed, covalent attachment of the protein and possibly generate a disordered film. However, the presence of the irreversibly bound fraction shows that this strategy was not entirely successful, albeit an improvement over the thiol-capped SAM employed previously (Wood et al., 1997).

Other features of the DOPE-PDS:DOPC bilayer that differentiate it from the thiol-capped SAM are: 1) a 6.6-Å spacer arm links the PDS group to DOPE (Fig. 2), which therefore should cause the reactive group to project above the surface of the surrounding DOPC matrix. Since Cys-102 is not directly on the surface of yeast cyt *c* (Louie et al., 1988), the presence of the spacer arm may facilitate formation of a covalent bond between this residue and PDS. In contrast, a spacer arm was not present in the SAM architecture. 2) As the lipid molecules in a liquid-crystalline lipid bilayer are likely to be less tightly packed than the alkyl chains of a silane-based SAM, the bilayer presents a softer adsorbent surface to a protein adsorbate. Consequently, cyt *c* molecules adsorbed to the DOPC:DOPE-PDS bilayer may partially penetrate into the bilayer, as reported by for horse heart cyt *c* adsorbed to phosphatidylglycerol bilayers (Heimburg and Marsh, 1995). Partial penetration, possibly accompanied by structural changes (Heimburg and Marsh, 1993; Muga et al., 1991), could be a mechanism contributing to the formation of the irreversibly bound fraction of the protein film. On the other hand, cyt *c* molecules that did penetrate into the bilayer and interact noncovalently with lipid headgroups and acyl chains probably would not readily desorb when soaked in a combination of salt and DTT. Thus, the ~70% of the protein molecules that were desorbed under these conditions were probably not inserted into the bilayer. 3) Lateral diffusion of lipids, and probably of cyt *c* molecules linked to DOPE-PDS, occurs in the bilayer-based architecture. Lateral diffusion may have facilitated lateral packing interactions between immobilized cyt *c* molecules, leading to a more ordered protein film, as has been observed for streptavidin bound to a biotin-capped lipid film (Darst et al., 1991). In contrast, lateral diffusion of the alkyl chains in a silane-based SAM is restricted by intermolecular cross-linking between silanols, although the protein molecules may undergo relatively slow diffusion when adsorbed to the SAM surface (Tilton et al., 1990).

## CONCLUSIONS

Yeast cyt *c* was immobilized via a site-directed, disulfide bonding strategy on phospholipid bilayers bearing pyridine disulfide groups. Orientation distribution measurements showed that the porphyrin groups in the protein layer exhibited a relatively high degree of macroscopic orientation, and provide direct evidence that this immobilization strategy can produce an ordered protein film.

Desorption experiments were used to assess the types of the binding interactions that occurred between cyt *c* and the lipid bilayers. The results showed that a large fraction of the immobilized protein molecules in the film were disulfide bonded to the bilayer. However, a fraction of the protein film was irreversibly immobilized, presumably via nonspecific interactions, and exhibited a broad orientation distribution. Thus, the use of site-directed immobilization to a LB film architecture to produce an ordered protein array was not entirely successful but certainly more so than a previous study in which yeast cyt *c* was deposited on a SAM architecture (Wood et al., 1997). Finally, it must be noted that despite the encouraging results of this study, an inherent lack of stability and the difficulty of fabrication are major limitations of LB film architectures for biomolecular device fabrication.

We thank Andrew Back for help with computer modeling and John Lee, Laurie Wood, and Sergio Mendes for helpful discussions.

This work was supported by National Science Foundation Grant CHE-9403896 and National Institutes of Health Grant R29 GM50299.

## REFERENCES

Alhmed, S. M. 1966. Studies of the dissolution of oxide surfaces at the liquid-solid interface. *Can. J. Chem.* 44:1663–1670.

Arnold, M. A., and M. E. Meyerholf. 1988. Recent advances in the development and analytical applications of biosensing probes. *CRC Crit. Rev. Anal. Chem.* 20:149–196.

Blankenburg, R., P. Meller, H. Ringsdorf, and C. Salesse. 1989. Interaction between biotin lipids and streptavidin in monolayers: formation of oriented two-dimensional protein domains induced by surface recognition. *Biochemistry.* 28:8214–8221.

Brayer, G. D., and M. E. P. Murphy. 1996. Structural studies of eukaryotic cytochromes *c*. *In* Cytochrome *c*: A Multidisciplinary Approach, Ch. 3. R. A. Scott, and A. G. Mauk, editors. University Science, Sausalito.

Cullison, J. K., F. M. Hawkridge, N. Nakashima, and S. Yoshikawa. 1994. A study of cytochrome *c* oxidase in lipid bilayer membranes on electrode surfaces. *Langmuir.* 10:877–882.

Darst, S. A., M. Ahlers, P. H. Meller, E. W. Kubalek, R. Blankenburg, H. Ribi, H. Ringsdorf, and R. D. Kornberg. 1991. Two-dimensional crystals

of streptavidin on biotinylated lipid layers and their interactions with biotinylated macromolecules. *Biophys. J.* 59:387–396.

Darst, S. A., C. R. Robertson, and J. A. Berzofsky. 1988. Adsorption of the protein antigen myoglobin affects the binding of conformation-specific monoclonal antibodies. *Biophys. J.* 53:533–539.

Demel, R. A., W. Jordi, H. Lambrecht, H. van Damme, R. Hovius, and B. de Kruijff. 1989. Differential interactions of apo- and holocytochrome *c* with acidic membrane lipids in model systems and the implications for their import into mitochondria. *J. Biol. Chem.* 264:3988–3997.

De Ruiter, G. A., P. Smid, J. H. Van Boom, and F. M. Rombouts. 1992. Detection of fungal carbohydrate antigens by high-performance immunoaffinity chromatography using a protein A column with covalently linked immunoglobin G. *J. Chromatogr.* 584:69–75.

Edmiston, P. L., J. E. Lee, S. S. Cheng, and S. S. Saavedra. 1997. Molecular orientation distributions in protein films. I. Cytochrome *c* adsorbed to substrates of variable surface chemistry. *J. Am. Chem. Soc.* 119:560–570.

Edmiston, P. L., J. E. Lee, L. L. Wood, and S. S. Saavedra. 1996. Dipole orientation distributions in Langmuir-Blodgett films by planar waveguide linear dichroism and fluorescence anisotropy. *J. Phys. Chem.* 100:775–784.

Firestone, M. A., M. L. Shank, S. G. Sligar, and P. W. Bohn. 1996. Film architecture in biomolecular assemblies: effect of linker on the orientation of genetically engineered surface-bound proteins. *J. Am. Chem. Soc.* 118:9033–9041.

Fraaije, J. G. E. M., J. M. Kleijn, M. van der Graaf, and J. C. Dijt. 1990. Orientation of adsorbed cytochrome *c* as a function of the electrical potential of the interface studied by total internal reflection fluorescence. *Biophys. J.* 57:965–975.

Hage, D. S., and P. C. Kao. 1991. High-performance immunoaffinity chromatography and chemiluminescent detection in the automation of a parathyroid hormone sandwich immunoassay. *Anal. Chem.* 63:586–595.

Hamachi, I., S. Noda, and T. Kunitake. 1991. Functional conversion of myoglobin bound synthetic bilayer membranes: from dioxygen storage protein to redox enzyme. *J. Am. Chem. Soc.* 113:9625–9630.

Heimburg, T., and D. Marsh. 1993. Investigation of secondary and tertiary structural changes of cytochrome *c* in complexes with anionic lipids using amide hydrogen exchange measurements: an FTIR study. *Biophys. J.* 65:2048–2417.

Heimburg, T., and D. Marsh. 1995. Protein surface-distribution and protein-protein interactions in the binding of peripheral proteins to charged lipid membranes. *Biophys. J.* 68:536–546.

Helm, C. A., H. Möhwald, K. Kjaer, and J. Als-Anielsen. 1987. Phospholipid monolayers between fluid and solid states. *Biophys. J.* 52:381–390.

Huang, X., J. M. Kovaleski, and M. J. Wirth. 1996. Spectroscopic probing of mixed-mode adsorption of $Ru(bpy)_3^{2+}$ to silica. *Anal. Chem.* 68: 4119–4123.

Kohr, J., and H. Engelhardt. 1993. Characterization of quartz capillaries for capillary electrophoresis. *J. Chromatogr.* 652:309–316.

Koppenol, W. H., and E. Margoliash. 1982. The asymmetric distribution of charges on the surface of horse cytochrome *c. J. Biol. Chem.* 257: 4426–4437.

Louie, G. V., W. L. B. Hutcheon, and G. D. Brayer. 1988. Yeast iso-1-cytochrome *c*: a 2.8 Å resolution three-dimensional structure determination. *J. Mol. Biol.* 199:295–314.

Luzzati, V. 1968. X-ray diffraction studies of lipid-water systems. *In* Biological Membranes. D. Chapman, editor. Academic Press, Inc., New York. 71–123.

Martin, F. J., W. L. Hubbell, and D. Papahadjopoulos. 1981. Immunospecific targeting of liposomes to cells: a novel and efficient method for covalent attachment of Fab′ fragments via disulfide bonds. *Biochemistry.* 20:4229–4238.

Mayo, S. L., B. D. Olafson, W. A. Goddard III. 1990. DREIDING: A generic force field for molecular simulations. *J. Phys. Chem.* 94: 8897–8909.

Mrksich, M., J. R. Grunwell, and G. M. Whitesides. 1995. Biospecific adsorption of carbonic anhydrase to self-assembled monolayers of alkanethiolates that present benzenesulfonamide groups on gold. *J. Am. Chem. Soc.* 117:12009–12010.

Müller, W., H. Ringsdorf, E. Rump, G. Wildburg, X. Zhang, L. Angermaier, W. Knoll, M. Liley, and J. Spinke. 1993. Attempts to mimic docking processes of the immune systems: recognition induced formation of protein multilayers. *Science.* 262:1706–1708.

Muga, A., H. H. Mantsch, and W. K. Surewicz. 1991. Membrane binding induces destabilization of cytochrome *c* structure. *Biochemistry.* 30: 7219–7224.

Pachence, J. M., S. Amador, G. Maniara, J. Vanderkooi, P. L. Dutton, and J. K. Blasie. 1990. Orientation and lateral mobility of cytochrome *c* on the surface of ultrathin lipid multilayer films. *Biophys. J.* 58:379–389.

Pachence, J. M., and J. K. Blasie. 1991. Structural investigation of the covalent and electrostatic binding of yeast cytochrome *c* to the surface of various ultrathin lipid multilayers using x-ray diffraction. *Biochem. J.* 59:894–900.

Prokop, L. A., R. M. Strongin, A. B. Smith III, J. K. Blasie, L. J. Peticolas, and J. C. Bean. 1995. Vectorially oriented monolayers of detergent-solubilized $Ca^{2+}$-ATPase from sarcoplasmic reticulum. *Biophys. J.* 70: 2131–2143.

Quinn, P. J., and R. M. C. Dawson. 1969. Interactions of cytochrome *c* and [$^{14}$C]carboxymethylated cytochrome *c* with monolayers of phosphatidylcholine, phosphatidic acid ad cardiolipin. *Biochem. J.* 115:65–75.

Robinson, A. B., and M. D. Kamen. 1968. *In* Structure and Function of Cytochromes. K. Okunuki, M. D. Kamen, and I. Sekuzu, editors. University Park Press, Baltimore. 383–387.

Salamon, Z., and G. Tollin. 1996. Surface plasmon resonance studies of complex formation between cytochrome *c* and bovine cytochrome *c* oxidase incorporated into a supported planar lipid bilayer. I. Binding of cytochrome *c* to cardiolipin/phosphatidylcholine membranes in the absence of oxidase. *Biophys. J.* 71:848–857.

Sankaram, M. B., and D. Marsh. 1993. Protein-lipid interactions with peripheral membrane proteins. *In* Protein-Lipid Interactions. A. Watts, editor. Elsevier, Amsterdam. 127–162.

Schindler, P. W., B. Furst, R. Dick, and P. Wolf. 1976. Ligand properties of surface silanol groups. *J. Colloid Interface Sci.* 55:469–475.

Smith, P. K., R. I. Krohn, G. T. Hermanson, A. K. Mallia, F. H. Gartner, M. D. Provenzano, E. K. Fujimoto, N. M. Goeke, B. J. Olson, and D. C. Klenk. 1985. Measurement of protein using bicinchoninic acid. *Anal. Biochem.* 150:76–85.

Song, S., R. A. Clark, E. F. Bowden, and M. J. Tarlov. 1993. Characterization of cytochrome *c*/alkanethiolate structures prepared by self-assembly on gold. *J. Phys. Chem.* 97:6564–6572.

Swalen, J. D., D. L. Allara, J. D. Andrade, E. A. Chandross, S. Garoff, J. Israelchvili, T. J. McCarthy, R. Murray, R. F. Pease, J. F. Rabolt, K. J. Wynne, and H. Yu. 1987. Molecular monolayers and films. *Langmuir.* 3:932–950.

Tamm, L. K., and H. M. McConnell. 1985. Supported phospholipid bilayers. *Biophys. J.* 47:105–113.

Tarlov, M. J., and E. F. Bowden. 1991. Electron-transfer reaction of cytochrome *c* adsorbed on carboxylic acid terminated alkanethiol monolayer electrodes. *J. Am. Chem. Soc.* 113:1847–1849.

Tilton, R. D., C. R. Robertson, and A. P. Gast. 1990. Lateral diffusion of bovine serum albumin adsorbed at the solid-liquid interface. *J. Colloid Interface Sci.* 137:192–203.

Timbs, M. M., and N. L. Thompson. 1990. Slow rotational mobilities of antibodies and lipids associated with substrate-supported phospholipid monolayers as measured by polarized fluorescence photobleaching recovery. *Biophys. J.* 56:413–428.

Wiener, M. C., and S. H. White. 1992. Structure of a fluid dioleoylphosphatidylcholine bilayer determined by joint refinement of x-ray and neutron diffraction data. III. Complete structure. *Biophys. J.* 61: 434–447.

Wood, L. L., S. S. Cheng, P. L. Edmiston, and S. S. Saavedra. 1997. Molecular orientation distributions in protein films. II. Site-directed immobilization of yeast cytochrome *c* on thiol-capped, self-assembled monolayers. *J. Am. Chem. Soc.* 119:571–576.

Yang, L., S. S. Saavedra, N. R. Armstrong, and J. Hayes. 1994. Fabrication and characterization of low-loss, sol-gel planar waveguides. *Anal. Chem.* 66:1254–1263.

Yue, B. Y., C. M. Jackson, J. A. G. Taylor, J. Minigins, and B. A. Pethica. 1976. Phospholipid monolayers at non-polar oil/water interfaces. *J. Chem. Soc. Faraday Trans. 1.* 72:2685–2693.